Thermodynamic Studies of the Core Histones: Stability of the Octamer Subunits Is Not Altered by Removal of Their Terminal Domains†

Vassiliki Karantza, Ernesto Freire, and Evangelos N. Moudrianakis*

Department of Biology, The Johns Hopkins University, Baltimore, Maryland 21218

Received May 17, 2001; Revised Manuscript Received August 6, 2001

ABSTRACT: We have investigated the role of the labile terminal domains of the core histones on the stability of the subunits of the protein core of the nucleosome by studying the thermodynamic behavior of the products of limited trypsin digestion of these subunits. The thermal stabilities of the truncated H2A−H2B dimer and the truncated (H3−H4)/$(H3−H4)_2$ system were studied by high-sensitivity differential scanning calorimetry and circular dichroism spectroscopy. The thermal denaturation of the truncated H2A−H2B dimer at pH 6.0 and low ionic strength is centered at 47.3 °C. The corresponding enthalpy change is 35 kcal/mol of 11.5 kDa monomer unit, and the heat capacity change upon unfolding is 1.2 kcal/(K mol of 11.5 kDa monomer unit). At pH 4.5 and low ionic strength, the truncated (H3−H4)/$(H3−H4)_2$ system, like its full-length counterpart, is quantitatively dissociated into two truncated H3−H4 dimers. The thermal denaturation of the truncated H3−H4 dimer is characterized by the presence of a single calorimetric peak centered at 60 °C. The enthalpy change is 25 kcal/mol of 10 kDa monomer unit, and the change in heat capacity upon unfolding is 0.5 kcal/(K mol of 10 kDa monomer unit). The thermal stabilities of both types of truncated dimers exhibit salt and pH dependencies similar to those of the full-length proteins. Finally, like their full-length counterparts, both truncated core histone dimers undergo thermal denaturation as highly cooperative units, without the involvement of any significant population of melting intermediates. Therefore, removal of the histone "tails" does not generally affect the thermodynamic behavior of the subunits of the core histone complex, indicating that the more centrally located regions of the histone fold and the extra-fold structured elements are primarily responsible for their stability and responses to parameters of their chemical microenvironment.

The repeating structural unit of chromatin, the nucleosome, is a complex between DNA and the core histone proteins. Two copies of each of the histones H2A, H2B, H3, and H4 are assembled in an octameric structure (originally proposed by Kornberg) (*1*) around which 146 bp of DNA are wrapped and form the nucleosome core particle (*2*). Earlier structural investigations focused on the thermal denaturation of chromatin and nucleosomes, and analyzed the overall nature of association of the core histone octamer with DNA (*3*−*8*). The thermodynamic studies of subunits of the protein core of the nucleosome have extended our understanding of the behavior of this system (*9*, *10*).

More recent investigations have focused on the role of the amino-terminal domains (ATDs) of the core histones, i.e., the histone "tails", in the stabilization of the core particle, the interaction of nucleosomes with nonhistone nucleosomal proteins, and the formation of higher order chromatin structures (*11*−*13*) [reviewed by Annunziato and Hansen (*14*)]. These ATDs contain a high concentration of positively charged residues and are the major sites of histone post-translational modifications, including acetylation, phosphorylation, and methylation [reviewed by Strahl and Allis and Wu and Grunstein (*15*, *16*)]. Such localized modifications have been implicated in the regulation of fundamental biological processes (*17*) such as DNA replication (*18*) and reviewed by Kaufman and Almouzni (*19*), transcription (*20*−*24*), chromatin remodeling (*25*, *26*), and the formation and regulation of oligonucleosomal arrays (*27*).

The importance of the terminal domains of the core histones on the integrity of the nucleosome has been probed by several methods, including selective proteolysis (truncation) (*11*, *13*, *18*, *23*, *28*−*32*, *33*) and immunochemistry (*34*−*36*).

In the present study, we investigate the contribution of the terminal regions of the core histones to the thermodynamic stability of the subunits of the protein components of the core particle. For this purpose, these subunits, i.e., the H2A−H2B dimer and the $(H3−H4)_2$ tetramer, were subjected to truncation by limited trypsin digestion. The thermal stabilities of the truncated complexes were studied as a function of ionic strength and pH, and were directly compared to the properties of their full-length counterparts. Our results clearly demonstrate that the thermodynamic stability of the core histone subunits derives from the structured elements of these protein assemblies, and in particular from the fundamental architectural motif of the histone fold. Furthermore, they show that the terminal

† This work was supported, in part, by a grant from the National Institutes of Health (RR-04328) and in part by a grant from the National Science Foundation (MCB-0091736).

* To whom correspondence should be addressed. Telephone (410) 516-7305. FAX (410) 516-6193. E-mail vanm@jhu.edu.

10.1021/bi0110140 CCC: $20.00
Published on Web 10/05/2001

domains make minimal, if any, contribution to the thermodynamic stability of the subunits of the core histone octamer. This is in stark contrast to the well-documented and multiple roles of these domains in the functional regulation of chromatin. Finally, this study extends our previous findings (*9*, *10*) and provides further support for our earlier proposals regarding the crucial role of the chemical microenvironment of chromatin on the modulation of its structure and, thus, its function.

MATERIALS AND METHODS

Isolation of Histones. Chicken erythrocyte histones were isolated by a modification of the salt extraction procedure previously used in this laboratory (*37*). The $(H3-H4)_2$ tetramer was efficiently separated from the H2A−H2B dimer on a CM-cellulose (Whatman CM-52) column equilibrated with 0.1 M potassium phosphate, 1 mM EDTA,[1] 0.5 M urea, pH 6.7, and eluted using a 0.1 to 0.6 M KCl stepwise gradient. All isolation steps were performed at 4 °C, with repeated additions of PMSF.

Trypsin Digestion. The core histone subunits were submitted to limited trypsin digestion as described by Hatch et al. (*28*). The H2A−H2B dimer or the $(H3-H4)/(H3-H4)_2$ system in 2 M NaCl, 1 mM EDTA, 10 mM HEPES, pH 7.5, were digested with trypsin at 5 μg/mL, for 4−6 h on ice, and the progress of the reaction was monitored by $NaDodSO_4$−polyacrylamide gel electrophoresis. When the characteristic "limit peptides" were obtained, the reaction was stopped by the addition of egg white trypsin inhibitor in a 20-fold molar excess over trypsin. The total incubation mixture was subsequently dialyzed against 0.1 M potassium phosphate, 1 mM EDTA, 0.5 M urea, pH 6.7, and chromatographed through a CM-cellulose (Whatman CM-52) column, to separate the histone complexes from the trypsin and the trypsin inhibitor. The truncated H2A−H2B dimer or the truncated $(H3-H4)/(H3-H4)_2$ system were recovered as sharp peaks at 0.4 or 1 M KCl, respectively.

Sample Preparation. The truncated H2A−H2B samples and the truncated $(H3-H4)/(H3-H4)_2$ samples were equilibrated by overnight dialysis into the desired pH and NaCl-containing buffers. The differential scanning calorimetry (DSC) experiment for the truncated H2A−H2B dimer was performed in a solution containing 25 mM NaCl, 10 mM imidazole, pH 6.0. Truncated H2A−H2B samples for the CD ionic strength experiments were prepared in solutions containing 0.001−2 M NaCl, 10 mM HEPES, pH 7.5. The CD pH series experiments for the truncated H2A−H2B dimer were performed in solutions containing 100 mM NaCl and ranging in pH from 3.5 to 9.5. The DSC experiment for the truncated H3−H4 dimer was performed in a solution containing 12.5 mM NaCl, 10 mM glycylglycine, pH 4.2. Truncated H3−H4 samples for the CD ionic strength experiments were prepared in solutions containing 5−50 mM NaCl, 10 mM MES, pH 4.5. The CD pH series experiments for the $(H3-H4)/(H3-H4)_2$ system were performed in solutions containing 50 mM NaCl and ranging in pH from 1.5 to 8.5. The buffers used for the pH series experiments were 10 mM glycine for pH 1.5−4.0, 10 mM MES for pH 4.5−5.5, 10 mM HEPES for pH 6.5−7.5, and 10 mM bicine for pH 8.5−9.5. Truncated H3−H4 samples for the CD measurements of the protein concentration series were prepared in 5 mM NaCl, 10 mM glycylglycine, pH 4.0. For the urea denaturation experiments, protein samples were dialyzed into 0.8 M NaCl, 0.5 mM EDTA, 10 mM HEPES, pH 7.5 and, subsequently, denatured by the addition of 0.8−6.0 M urea, in 0.4 M increments. Protein concentrations used were 2 mg/mL for the trypsin digestions; 2.3−2.5 mg/mL for the DSC experiments; 0.3 mg/mL for the CD ionic strength and pH experiments; 0.15−1.42 mg/mL for the CD protein concentration series; 1 mg/mL for the small-zone exclusion chromatography experiments; and 0.25 mg/mL for the CD urea denaturation experiments. The concentrations were determined spectrophotometrically immediately prior to performing each experiment as previously described (*38*). Protein purity was assayed on 20% acrylamide−0.1% $NaDodSO_4$−polyacrylamide gels (*39*). Proteins were visualized by bathing the gels in 40% ethanol, 5% acetic acid, and 0.1% Coomassie Brilliant Blue R. Gels were subsequently destained with 20% ethanol, 5% acetic acid.

Differential Scanning Calorimetry. The experiments were performed at a scanning rate of 60 °C/h in the DASM4 and nanoDSC differential scanning microcalorimeters (Biocalorimetry Center, The Johns Hopkins University, Baltimore, MD). The calorimetric unit was interfaced to an IBM PC microcomputer using an analog−digital converter (Data Translation DT-2801) for automatic data collection and analysis. The sample and the reference solution were properly degassed and carefully loaded into the calorimeter to eliminate bubbling effects. To test for the ability of the protein to renature, the sample was cooled at the end of the first scan, allowed to reequilibrate to the starting temperature, and then scanned again. The percent renaturation is expressed as the ΔH_{cal} of the second scan divided by that of the first. The excess heat capacity function was analyzed after normalization and baseline subtraction using programs developed at the Biocalorimetry Center.

Circular Dichroism. All circular dichroism (CD) measurements were performed in a Jasco J-710 spectropolarimeter interfaced to an IBM PC microcomputer for automatic data collection and analysis. Temperature scans were performed by scanning continuously from 6 to 85 °C in a 1-mm rectangular quartz cell (Hellma Scientific). Temperature was controlled using a Haake PG20 temperature programmer interfaced to a Haake F3 circulating water bath, with a rate of increase in temperature of 60 °C/h. Temperature was monitored using a Microtherm 1006 thermometer and an S/N 117C temperature probe just outside of the sample cell. Data were collected using the time scan mode within the J-710 software package. The ellipticity at 222 nm was recorded every 20 s with a response time of 1 s and a bandwidth of 1 nm. The ellipticity and the temperature were manually recorded at discrete intervals of 5 °C, and intermediate temperatures were interpolated for every intervening ellipticity reading to yield a complete description of Θ_{222} vs

[1] Abbreviations: ΔC_p, observed difference in the heat capacity between the unfolded and the native states; ΔH, enthalpy change; ΔH_{cal}, calorimetric enthalpy change, ΔG, free energy of stabilization; ΔS, entropy change; $[\Theta]_\lambda$, molar ellipticity, in deg cm^2 dmol^{-1}; CD, circular dichroism; CM, carboxymethyl cellulose; DSC, differential scanning calorimetry; EDTA, ethylenediamine-tetraacetic acid; HEPES, *N*-(2-hydroxyethyl)piperazine-*N*′-2-ethanesulfonic acid; kDa, kilodaltons; MES, 2-(*N*-morpholino)ethanesulfonic acid; $NaDodSO_4$, sodium dodecyl sulfate; PMSF, phenylmethanesulfonyl fluoride; SSR, sum of the squared residuals of the fit; T_m, melting temperature.

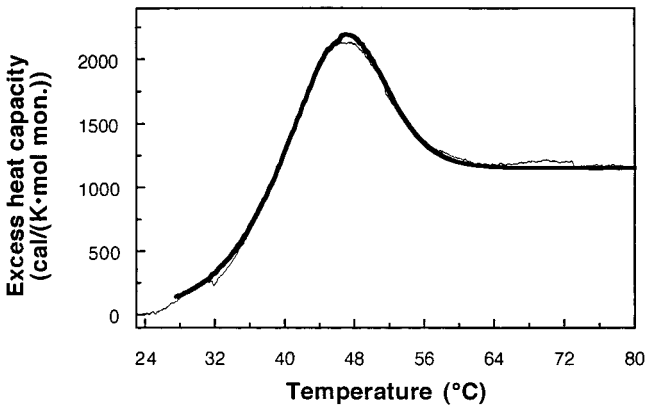

FIGURE 1: Excess heat capacity of the truncated H2A−H2B dimer as a function of temperature in 25 mM NaCl, 10 mM imidazole, pH 6.0, using DSC. The protein concentration was 216 μM 11.5-kDa monomer unit. The thin solid line represents experimental data, whereas the thick solid line represents the theoretical curve generated according to the two-state model discussed in the Statistical Thermodynamic Analysis section.

temperature. Ellipticity readings were normalized to fraction unfolded using the equation:

$$P_u=(\Theta - \Theta_N)/(\Theta_D - \Theta_N)$$

where Θ_D and Θ_N represent the ellipticity values for the fully unfolded and fully folded state at each temperature, as calculated from the slopes of the baselines preceding and following the transition region.

Small-Zone Exclusion Chromatography. The comparison of the self-associative properties between the truncated and the full-length H3−H4 complexes at pH 4.5 was performed by the small-zone exclusion chromatography technique (*37*), using a Sephadex G-100 column maintained at a flow rate of 15 mL/h. The experiments were performed at 4 °C, and 2 mL aliquots of the sample solutions in 25 mM NaCl, 10 mM glycylglycine, pH 4.5, were loaded on the column. For the column elution profiles, 4-mL fractions were collected.

RESULTS

Limited trypsin digestion of chromatin gives rise to a stable population of truncated core histones, also called "limit peptides" (*40*). The same set of truncated histone chains is also produced if the substrate is nuclei (*41*), native core particles (*42*), reconstituted core particles, or the core histone octamer in 2 M NaCl, pH 7.5 (*43*). Upon trypsin digestion, all core histones lose N-terminal residues, while H2A (and sometimes H3) also loses C-terminal residues. In the present study, the subunits of the core histone octamer, i.e., the H2A−H2B dimer and the $(H3-H4)_2$ tetramer, were individually subjected to trypsin digestion in neutral solutions of 2 M NaCl according to the method developed and calibrated by Hatch et al. (*28*). Electrophoresis in $NaDodSO_4$−polyacrylamide gels established that reproducible sets of stable truncated, limit peptides closely resembling the tryptic peptides of the earlier studies were produced (data not shown). By analogy to the size of the limit peptides obtained from chromatin (*41*, *44*, *45*), molecular masses of about 23 and 20 kDa were assigned to the truncated H2A−H2B dimer and the truncated H3−H4 dimer, respectively.

Salt Concentration Dependence of the Melting of the Truncated H2A−H2B Dimer. The thermal stability of the

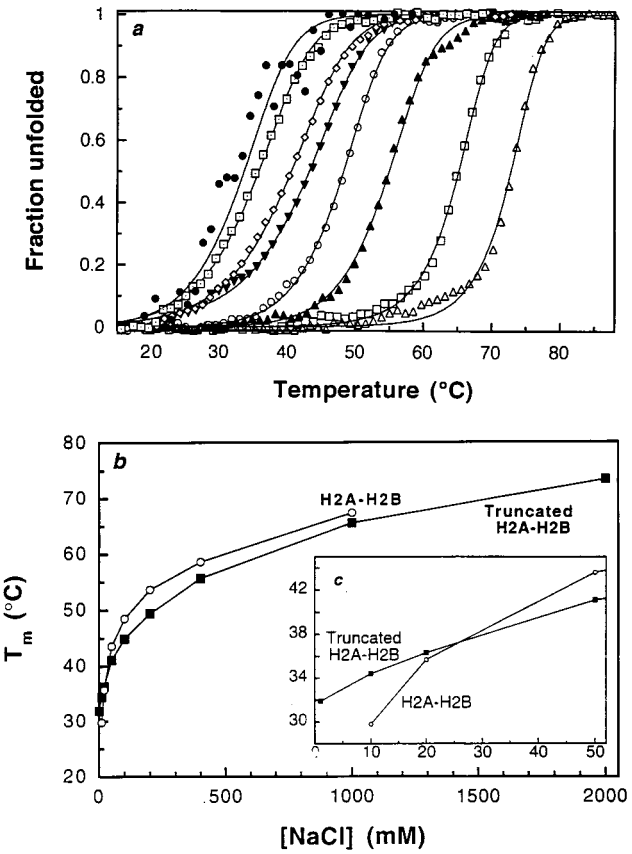

FIGURE 2: (a) Fraction of truncated H2A−H2B dimer unfolded at increasing ionic strength as a function of temperature. The NaCl concentrations are 11 mM (filled circles), 21 mM (open squares with point), 51 mM (open diamonds), 100 mM (filled inverted triangles), 200 mM (open circles), 400 mM (filled triangles), 1 M (open squares), and 2 M (open triangles). Experiments were performed in 0.1 mM EDTA, 10 mM HEPES, pH 7.5. The protein concentration was kept constant at 26 μM 11.5-kDa monomer unit. Fraction unfolded was monitored by the ellipticity at 222 nm using CD spectroscopy. Experimental data are represented by symbols. Theoretical curves generated with the parameters shown in Table 1 are represented by solid lines. (b) Melting temperatures of the truncated (filled squares) and the full-length (open circles) H2A−H2B dimers as a function of ionic strength using CD spectroscopy. T_m represents the temperature at which the fraction unfolded is equal to 0.5. (c) Enlarged representation of the 0−50 mM ionic strength portion of panel b.

truncated H2A−H2B dimer was studied by DSC and CD spectroscopy. At 25 mM NaCl and pH 6.0, the unfolding transition of the truncated H2A−H2B dimer is characterized by the presence of a single calorimetric peak centered at 47.3 °C, an enthalpy change of about 35 kcal/mol of 11.5 kDa monomer unit, and a heat capacity difference between the unfolded and the native states (ΔC_p) of about 1.2 kcal/(K·mol of 11.5 kDa monomer unit) (Figure 1). Because the truncated H2A−H2B dimer exhibited increased aggregation near neutrality at the high protein concentrations required for DSC, the calorimetric experiment was performed at pH 6.0 instead of pH 7.5, where most of the DSC data for the full-length protein were collected (*9*).

The effect of salt concentration on the stability of the truncated H2A−H2B dimer was investigated using a family of melting profiles monitored by CD spectroscopy at constant wavelength (CD melting profiles). The experiments were performed on samples dialyzed against 0.001−2.0 M NaCl at neutrality (Figure 2a). As shown in Figure 2b, the stability

Table 1: Thermodynamic Parameters of Truncated H2A−H2B Unfolding as a Function of Ionic Strength

	[NaCl] (mM)	T_m (°C)	$T°$ (°C)[a]	$\Delta H(T°)$ [kcal (mol mon.)$^{-1}$]	$\Delta S(T°)$ [cal (K mol mon.)$^{-1}$]	$\Delta C_p(T°)$ [kcal (K mol) mon.)$^{-1}$]	SSR[b]
DSC[c]	25	47.3	63.5	54.3	161	1.2	40
CD[d]	1	31.9	54.5	58.5	178	1.0	0.08
	11	34.4	55.7	61.2	186	1.0	0.06
	21	36.3	58.4	61.3	185	1.1	0.04
	51	41.1	62.8	62.7	187	1.1	0.03
	100	44.9	67.6	64.4	190	1.2	0.03
	200	49.4	71.3	66.8	194	1.2	0.03
	400	55.7	75.4	72.5	208	1.3	0.03
	1000	65.6	82.6	85.0	239	1.4	0.02

[a] $T°$ is the reference temperature at which the intrinsic free energy $\Delta G°$ is equal to zero. [b] SSR is the sum of the squared residuals of the fit. [c] pH 6.0. [d] pH 7.5

of the truncated H2A−H2B dimer increases as a function of ionic strength, with the transition temperature increasing from 31.9 °C at 1 mM NaCl to 89.7 °C at 2 M NaCl. The enthalpy change associated with the unfolding transition also increases as a function of salt concentration, ranging from 37 kcal/mol of 11.5 kDa monomer at 1 mM NaCl to 65 kcal/mol of 11.5 kDa monomer at 2 M NaCl (Table 1). The salt concentration dependence of the stability of the truncated H2A−H2B dimer closely parallels the corresponding behavior of the full-length protein (*9*). For a direct comparison, a series of CD temperature scans at very low ionic strength (0−25 mM NaCl) in neutrality was performed for the full-length H2A−H2B dimer. The results are summarized in Figure 2b. The truncated H2A−H2B dimer is only marginally less stable than the full-length complex at 50 mM NaCl and higher salt concentrations, whereas it is slightly more stable than its full-length counterpart at extremely low salt concentrations (up to 25 mM NaCl), as shown in greater detail in the inset of Figure 2b. The increased stabilization of the truncated protein at very low ionic strength is also reflected in the fact that the truncated H2A−H2B dimer exhibits a measurable unfolding transition in as low as 1 mM NaCl, whereas the full-length complex requires a minimum of 10 mM NaCl.

pH Dependence of the Melting of the Truncated H2A−H2B Dimer. The thermal unfolding behavior of the truncated H2A−H2B dimer was examined in low ionic strength solutions ranging in pH from 2.5 to 8.5 (the protein precipitated upon heating at pH 9.5). A family of thermal denaturation profiles was obtained by CD spectroscopy, as shown in Figure 3a. The T_m of the truncated H2A−H2B dimer remains essentially constant between pH 5.5 and 8.5 (at about 47 °C), whereas it decreases below pH 5.0. The decrease in T_m, although initially small, becomes pronounced at pH 3.5 (Figure 3b). Below pH 3.0, the truncated H2A−H2B dimer is apparently unfolded at all temperatures, as no unfolding transition is measurable. The enthalpy change associated with the unfolding transition follows a similar pattern in that it remains essentially constant between pH 6.0 and 8.5 (at about 42 kcal/mol of 11.5 kDa monomer), whereas it decreases below pH 5.0 (Table 2). As summarized in Figure 3b, the truncated H2A−H2B dimer exhibits similar stability to the full-length protein around neutrality, whereas it becomes more stable than its full-length counterpart at low pH. As shown earlier (*9*), the T_m of the full-length H2A−H2B dimer is essentially constant between pH 6.5 and 9.5, whereas it decreases substantially below pH 5.0, with the protein being completely denatured below pH 4.0.

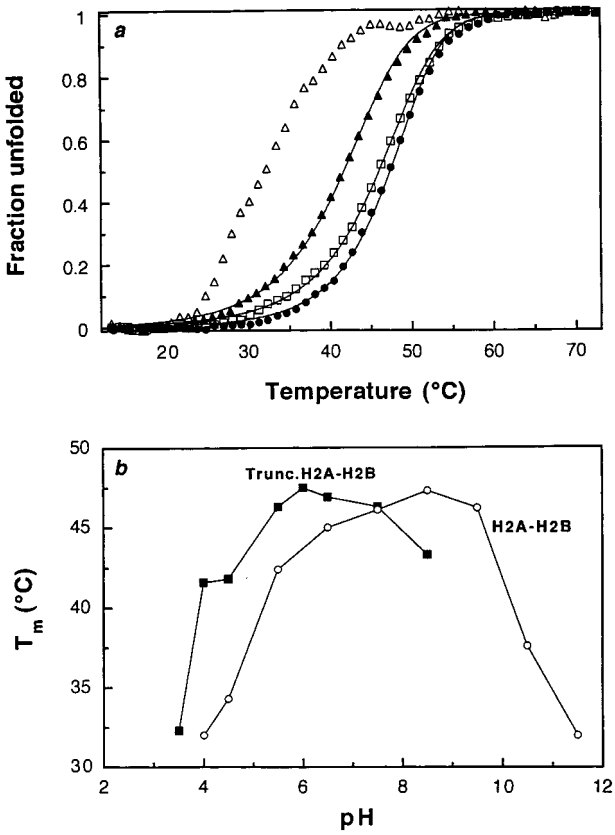

FIGURE 3: (a) Fraction of truncated H2A−H2B dimer unfolded at different pH values as a function of temperature. The pH values are 3.5 (open triangles), 4.5 (filled triangles), 5.5 (open squares), and 6.0 (filled circles). Experiments were performed in 100 mM NaCl, 10 mM appropriate pH buffer (see Materials and Methods). The protein concentration was kept constant at 28 μM 11.5-kDa monomer unit. The fraction unfolded was monitored by the ellipticity at 222 nm using CD spectroscopy. Experimental data are represented by symbols. Theoretical curves generated with parameters shown in Table 2 are represented by solid lines. (b) Melting temperatures of the truncated (filled squares) and the full-length (open circles) H2A−H2B dimers as a function of pH using CD spectroscopy. T_m represents the temperature at which the fraction unfolded is equal to 0.5.

Table 2: Thermodynamic Parameters of Truncated H2A−H2B Unfolding as a Function of pH

pH	T_m (°C)	$T°$ (°C)[a]	ΔH ($T°$) [kcal (mol monomer)$^{-1}$]	$\Delta S(T°)$ [cal (K mol monomer)$^{-1}$]	SSR[b]
3.5	32.3				
4.0	41.6	69.8	48.7	142	0.02
4.5	41.8	66.8	52.5	154	0.02
5.5	46.3	69.8	57.7	168	0.02
6.0	47.5	68.5	63.4	186	0.02
6.5	46.9	68.5	64.0	187	0.02
7.5	46.3	68.2	62.7	184	0.02
8.5	43.3	64.3	59.2	175	0.03

[a] $T°$ is the reference temperature at which the intrinsic free energy $\Delta G°$ is equal to 0. [b] SSR is the sum of the squared residuals of the fit.

CD experiments indicate that the pH-dependence of the α-helical content of the truncated H2A−H2B dimer follows a pattern that is consistent with the pH dependence of the T_m of the unfolding transition. The α-helical content is

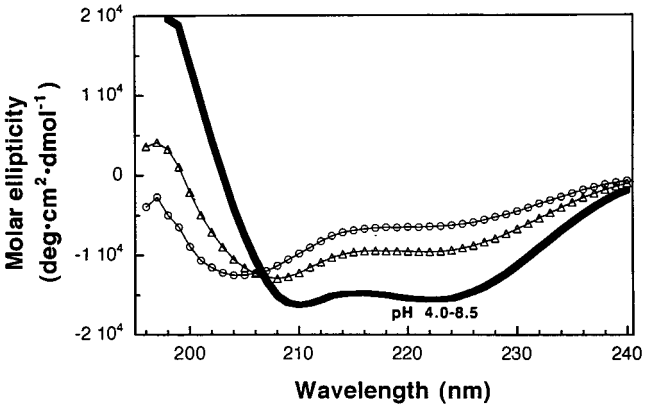

FIGURE 4: Far-UV CD spectra of the truncated H2A−H2B dimer at different pH values. Experiments were performed in 100 mM NaCl, 10 mM appropriate pH buffer. The protein concentration was kept constant at 28 μM 11.5-kDa monomer unit. The pH values are 4.0−8.5 (thick solid line), 3.5 (triangles), and 2.5 (circles).

maximum and essentially constant between pH 4.0 and 8.5, whereas it decreases substantially at pH 3.5. An even more radical decrease takes place at pH 2.5 (Figure 4). It should be noticed that a well-defined isodichroic point is observed at about 206 nm, which is characteristic of a system with only two, optically distinguishable, conformations.

Salt Concentration Dependence of the Melting of the Truncated H3−H4 Dimer. The self-associative properties of the truncated H3−H4 complex at pH 4.5 were compared to those of the full-length protein under similar conditions by small-zone exclusion chromatography. In an earlier study (*10*), it was documented that at pH 4.5 and low salt concentrations, the equilibrium $2(H3/H4) \leftrightarrow (H3/H4)_2$ is quantitatively shifted to the left, and the only molecular species detectable in solution is the H3/H4 dimer. Under similar conditions, the truncated H3−H4 protein elutes as a single peak, migrating slightly more slowly than the full-length H3−H4 dimer (data not shown). Therefore, the truncated H3−H4 protein quantitatively exists as a dimeric complex at pH 4.5, just like its full-length counterpart.

The reversible unfolding behavior of the truncated H3/H4 system was studied by DSC and CD spectroscopy under conditions that promote its separation into two truncated H3−H4 dimers, exactly as it was done for the full-length (H3−H4)/(H3−H4)$_2$ system (*10*). In both cases, the experimental conditions were chosen to ensure thermodynamic reversibility, as explained earlier (*10*). The unfolding transition of the truncated H3−H4 dimer at 12.5 mM NaCl and pH 4.2 is characterized by the presence of a single calorimetric peak centered at 60.3 °C (data not shown). The enthalpy change is about 25 kcal/mol of 10-kDa monomer unit, and the heat capacity difference between the unfolded and the native states (ΔC_p) is about 0.5 kcal/(K mol of 10-kDa monomer unit). The dependence of the stability of the truncated H3−H4 dimer on salt concentration was examined by CD spectroscopy in solutions ranging from 5 to 50 mM NaCl (Figure 5a). The stability of the truncated H3−H4 dimer increases as a function of salt concentration (Table 3). As shown in Figure 5b, the transition temperature increases from 41.3 °C at 5 mM NaCl to 49.7 °C at 25 mM NaCl, whereas it remains at 49.7 °C at 50 mM NaCl. The fact that there is not any additional apparent increase in the transition temperature upon increase of the salt concentration from 25 to 50 mM

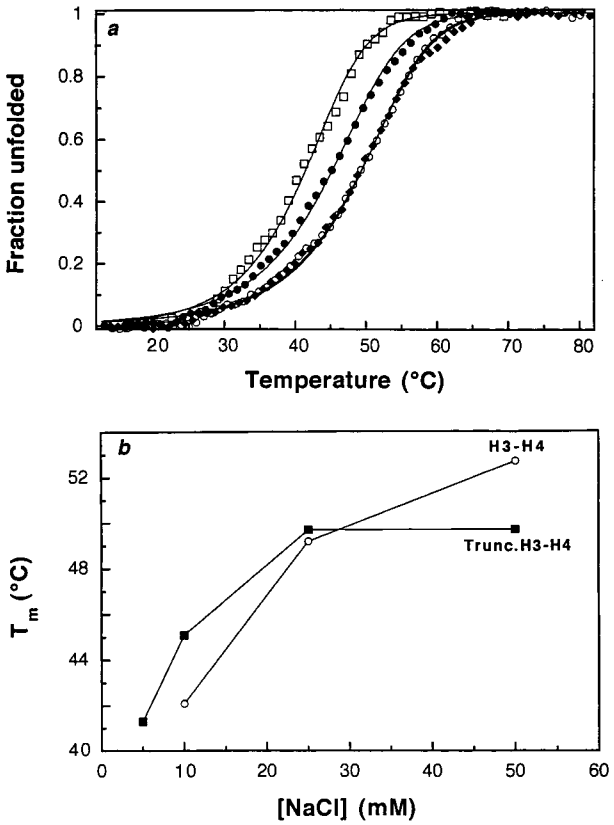

FIGURE 5: (a) Fraction of truncated H3−H4 dimer unfolded at increasing ionic strength as a function of temperature. The NaCl concentrations are 5 mM (open squares), 10 mM (filled circles), 25 mM (open circles), and 50 mM (filled diamonds). Experiments were performed in 10 mM MES, pH 4.5. The protein concentration was kept constant at 30 μM 10-kDa monomer unit. Fraction unfolded was monitored by the ellipticity at 222 nm. Experimental data are represented by symbols. Theoretical curves generated with the parameters shown in Table 3 are represented by solid lines. (b) Melting temperatures of the truncated (filled squares) and the full-length (open circles) H3−H4 dimers as a function of ionic strength using CD spectroscopy. T_m represents the temperature at which the fraction unfolded is equal to 0.5.

Table 3: Thermodynamic Parameters of Truncated H2A−H2B Unfolding as a Function of Ionic Strength

	[NaCl] (mM)	T_m (°C)	$T°$ (°C)[a]	ΔH ($T°$) [kcal (mol mon.)$^{-1}$]	$\Delta S(T°)$ [cal (K mol mon.)$^{-1}$]	$\Delta C_p(T°)$ [kcal (K mol) mon.)$^{-1}$]	SSR[b]
DSC[c]	12.5	60.3	86.3	38.2	106	0.5	17
CD[d]	5	41.3	69.8	46.5	136	0.5	0.04
	10	45.1	77.0	44.6	127	0.5	0.03
	25	49.7	81.7	44.7	126	0.5	0.02
	50	49.7	80.7	46.7	132	0.06	0.01

[a] $T°$ is the reference temperature at which the intrinsic free energy $\Delta G°$ is equal to zero. [b] SSR is the sum of the squared residuals of the fit. [c] pH 4.2 [d] pH 4.5

NaCl is most likely due to protein self-aggregation induced by salt. The earlier CD studies of the ionic effects on the stability of the full-length H3−H4 dimer (*10*) were performed in acetate buffers rather than NaCl. We now performed a series of similar CD experiments with the full-length H3−H4 dimer in NaCl solutions to obtain a more appropriate reference set of data. As summarized in Figure 5b, at very low ionic strength conditions, the truncated H3−H4 dimer is slightly more stable than its full-length counterpart. In

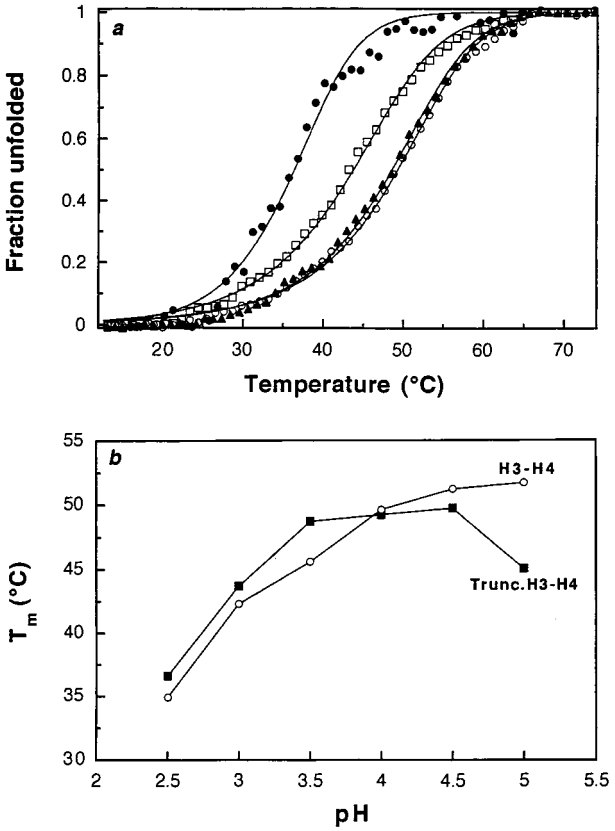

FIGURE 6: (a) Fraction of truncated H3−H4 dimer unfolded at different pH values as a function of temperature. The pH values are 2.5 (filled circles), 3.0 (open squares), 3.5 (filled triangles), and 4.5 (open circles). Experiments were performed in 50 mM NaCl, 10 mM appropriate pH buffer. The protein concentration was kept constant at 32 μM 10-kDa monomer unit. The fraction unfolded was monitored by the ellipticity at 222 nm using CD spectroscopy. Experimental data are represented by symbols. Theoretical curves generated with the parameters shown in Table 4 are represented by solid lines. (b) Melting temperatures of the truncated (filled squares) and the full-length (open circles) H3−H4 dimers as a function of pH using CD spectroscopy. T_m represents the temperature at which the fraction unfolded is equal to 0.5.

addition, the lowest salt concentration for which an unfolding transition can be measured by CD spectroscopy is 5 mM NaCl for the truncated H3−H4 dimer, as compared to 10 mM for the full-length protein. At salt concentrations greater than 25 mM NaCl, a comparison is no longer meaningful because of the apparent self-aggregative behavior of the truncated H3−H4 dimer.

The large apparent difference in the unfolding temperatures of the truncated H3−H4 dimer when determined by calorimetry as compared to that determined by CD under similar ionic strength conditions is well accounted for by the dependence of the melting temperature on protein concentration. The protein concentration for the DSC experiment was about eight times higher than that used for the CD experiments and, as expected for a system in which unfolding is coupled to dissociation, it resulted in a much higher transition temperature (see *Melting of the Truncated H3−H4 Dimer as a Function of Protein Concentration*).

pH-Dependence of the Melting of the Truncated H3−H4 Dimer. The thermal unfolding behavior of the truncated H3−H4 dimer at low ionic strength was examined by CD spectroscopy in solutions ranging in pH from 5.0 to 1.5, and the results are presented in Figure 6a. The T_m of the truncated

Table 4: Thermodynamic Parameters of Truncated H3−H4 Unfolding as a Function of pH

pH	T_m (°C)	$T°$ (°C)[a]	$\Delta H(T°)$ [kcal (mol monomer)$^{-1}$]	$\Delta S(T°)$ [cal (K mol monomer)$^{-1}$]	SSR[b]
2.5	36.6	65.3	41.7	123	0.07
3.0	43.7	76.2	42.5	122	0.04
3.5	48.7	79.5	45.7	130	0.03
4.0	49.2	81.2	44.8	126	0.02
4.5	49.7	80.7	46.7	132	0.01
5.0	45.1	76.1	40.6	116	0.02

[a] $T°$ is the reference temperature at which the intrinsic free energy $\Delta G°$ is equal to 0. [b] SSR is the sum of the squared residuals of the fit.

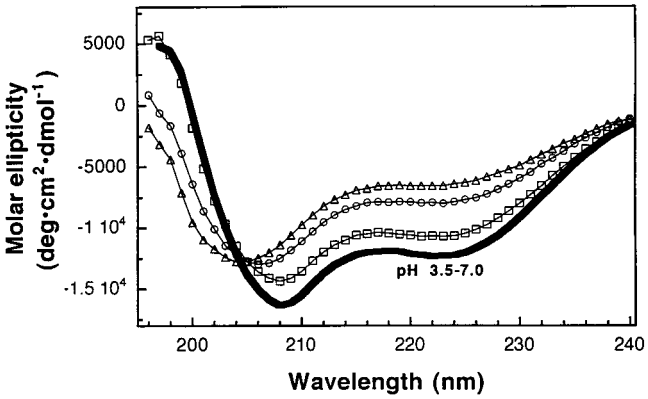

FIGURE 7: Far-UV CD spectra of the truncated (H3−H4)/(H3−H4)$_2$ system at different pH values. Experiments were performed in 50 mM NaCl, 10 mM appropriate pH buffer. The protein concentration was kept constant at 32 μM 10-kDa monomer unit. The pH values are 3.5−7.0 (thick solid line), 3.0 (squares), 2.5 (circles), and 1.5 (triangles).

H3−H4 dimer is essentially constant between pH 4.5 and 3.5 (at about 49 °C), whereas it progressively decreases below pH 3.5 (Figure 6b). At pH 1.5, no unfolding transition is detectable by CD spectroscopy. The apparent decrease in T_m observed at pH 5.0 is most likely due to self-aggregation of the truncated H3−H4 dimer induced by the increase in pH. The enthalpy change associated with the unfolding transition follows a similar pattern; it remains essentially constant between pH 4.5 and 3.5 (at about 28 kcal/mol of 10 kDa monomer unit), whereas it decreases below pH 3.5 (Table 4). As shown in Figure 6b, the pH dependence of the stability of the truncated H3−H4 dimer almost parallels the behavior exhibited by the full-length protein (*10*). At pH 4.0, the melting profiles for the truncated H3−H4 dimer and the full-length protein almost coincide. At pH 4.5, the full-length H3−H4 dimer is slightly more stable, whereas the situation is reversed below pH 4.0.

CD experiments indicate that the α-helical content of the truncated (H3−H4)/(H3−H4)$_2$ system as a function of pH follows a pattern that parallels and is consistent with the pH effect on the unfolding transition of the truncated H3−H4 dimer. As shown in Figure 7, the α-helical content of the truncated (H3−H4)/(H3−H4)$_2$ system is maximum and essentially constant between pH 7.0 and 3.5, whereas it slightly decreases at pH 3.0. An even more radical decrease in the α-helical content of the truncated H3−H4 dimer takes place in two successive steps, at pH 2.5 and 1.5, respectively. A single well-defined isodichroic point is observed at 204 nm, just like for the thermal denaturation of the full-length H3−H4 dimer (*10*).

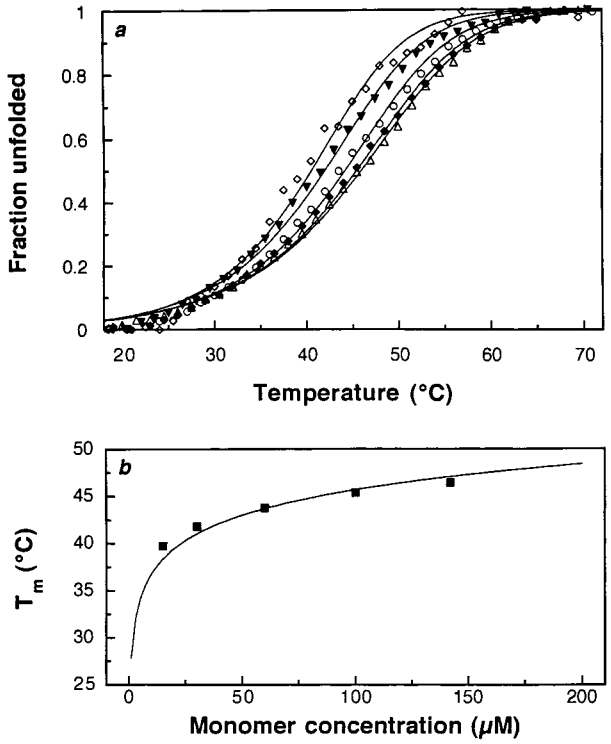

FIGURE 8: (a) Fraction of truncated H3−H4 dimer unfolded at increasing protein concentration as a function of temperature. The 10-kDa monomer unit concentrations are 15 μM (open diamonds), 30 μM (filled inverted triangles), 60 μM (open circles), 100 μM (filled diamonds), and 142 μM (open triangles). Experiments were performed in 5 mM NaCl, 10 mM glycylglycine, pH 4.0. The fraction unfolded was monitored by the ellipticity at 222 nm using CD spectroscopy. Experimental data are represented by symbols. Theoretical data generated with the parameters shown in Table 5 are represented by solid lines. (b) Melting temperatures of the truncated H3−H4 dimer as a function of monomer unit protein concentration. The squares represent CD data. The solid line is a best-fit logarithmic curve through theoretical transition temperatures, as calculated according to the model that predicts the coupling between dissociation and unfolding of the truncated H3-H4 dimer.

Melting of the Truncated H3−H4 Dimer as a function of Protein Concentration. The unfolding transitions for both the truncated H2A−H2B and H3−H4 dimers are coupled to the dissociation of the corresponding monomeric subunits. This is reflected in the slight asymmetry of the heat capacity function, which in both cases is skewed toward the low-temperature side of the transition (data not shown), as expected for a transition coupled to dissociation (*46*).

To confirm the coupling of unfolding and subunit dissociation for the truncated histone dimers, we also examined the effect of protein concentration on the transition temperature for the truncated H3−H4 dimer at pH 4.5 and very low ionic strength. In a series of thermal denaturation profiles monitored by CD spectroscopy (Figure 8a), the concentration of the protein was varied between 15 and 142 μM (as computed per 10 kDa monomer polypeptide subunit). As shown in Figure 8b, the transition temperature increases from 39.7 to 46.4 °C as the protein concentration increases from 15 to 142 μM, in agreement with a system that undergoes dissociation upon unfolding (*46*). Similar behavior was obtained with the truncated H2A−H2B dimer (data not shown). This is not surprising since both types of subunits share the histone fold and handshake motifs.

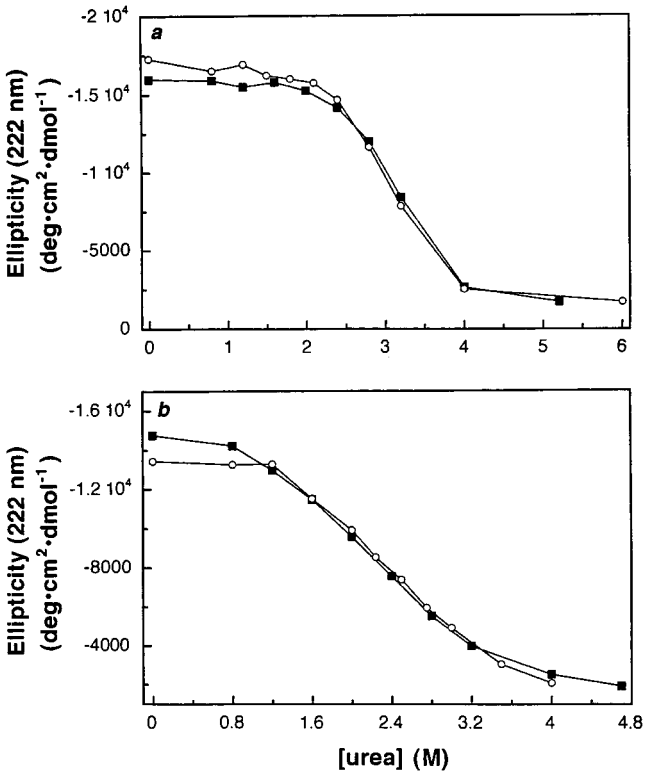

FIGURE 9: (a) Molar ellipticities of the truncated (filled squares) and the full-length (open circles) H2A−H2B dimers at 222 nm as a function of urea concentration. Far-UV CD experiments were performed in 0.8 M NaCl, 0.5 mM EDTA, 10 mM HEPES, pH 7.5. The protein concentrations were kept constant at 22 μM 11.5-kDa monomer unit and 18 μM 14-kDa monomer unit, respectively. (b) Molar ellipticities of the truncated (filled squares) and the full-length (open circles) (H3−H4)/(H3−H4)$_2$ systems at 222 nm as a function of urea concentration. Far-UV CD experiments were performed in 0.8 M NaCl, 0.5 mM EDTA, 10 mM HEPES, pH 7.5. The protein concentrations were kept constant at 25 μM 10-kDa monomer unit and 19 μM 13-kDa monomer unit, respectively.

Urea Denaturation. We further investigated the stabilities of the truncated H2A−H2B dimer and the truncated (H3−H4)/(H3−H4)$_2$ system and compared them to those of their corresponding full-length proteins. For this, urea denaturation experiments were monitored by CD spectroscopy in neutral solutions, containing 0.8 M NaCl and ranging in urea concentration from 0 to 6 M. The results are summarized in Figure 9a,b. As shown in Figure 9a, the truncated H2A−H2B dimer and the full-length H2A−H2B dimer exhibit almost identical denaturation profiles in increasing concentrations of urea, with the midpoint of the unfolding transitions at about 3.0 M urea. The truncated (H3−H4)/(H3−H4)$_2$ system and its full-length counterpart exhibit almost superimposable denaturation profiles (Figure 9b), with the midpoint of the unfolding transitions at about 2.4 M urea.

Statistical Thermodynamic Analysis. Just like for the full-length H2A−H2B dimer (*9*) and the full-length H3−H4 dimer (*9*), the corresponding truncated complexes behave as highly cooperative systems. The experimental data of the present study were analyzed in terms of the three-state formalism using a nonlinear least squares procedure (*47*), in a manner analogous to that described for the full-length H2A−H2B and H3−H4 dimers. In all cases examined, best fit was obtained without inclusion of any intermediate conformations. This indicates that each of the truncated

Table 5: Thermodynamic Parameters of Truncated H3−H4 Unfolding as a Function of Protein Concentration

10-kDa monomer conc (μM)	T_m (°C)	$T°$ (°C)[a]	$\Delta H(T°)$ [kcal (mol monomer)$^{-1}$]	$\Delta S(T°)$ [cal (K mol monomer)$^{-1}$]	SSR[b]
15	39.7	79.8	35.4	100	0.06
30	41.8	80.9	35.9	101	0.02
60	43.8	80.1	35.5	100	0.02
100	45.4	80.1	36.1	102	0.03
142	46.4	80.1	36.1	102	0.03

[a] $T°$ is the reference temperature at which the intrinsic free energy $\Delta G°$ is equal to 0. [b] SSR is the sum of the squared residuals of the fit.

dimers (H2A−H2B and H3−H4) underwent thermal denaturation by a two-state mechanism, in which the only states highly populated, at all temperatures, were native dimers and unfolded monomers. In this case, at any temperature the population of unfolded monomers is given by the equation (*48*):

$$P_U = P_X + P_Y = K[(K^2 + 4)^{1/2} - K]/2$$

where

$$K = \exp(-\Delta G°/RT)/(2[P_T])^{1/2}$$

and X and Y denote the two polypeptides comprising the dimer under study, i.e., the truncated H2A−H2B or the truncated H3−H4 dimer.

The equilibrium constant, K, is a function of the total protein concentration, $[P_T]$, as well as the intrinsic free energy of stabilization, $\Delta G°$. For convenience, all thermodynamic quantities are expressed on a mole of peptide chain basis. The intrinsic Gibbs energy is given by the standard equation:

$$\Delta G° = \Delta H°(T°) + \Delta C_p(T - T°) - T[\Delta S°(T°) + \Delta C_p \ln(T/T°)]$$

where by definition $T°$ is the temperature at which $\Delta G°$ is equal to zero. This temperature is independent of concentration and should not be confused with the transition temperature, which is concentration dependent. Contrary to the example of a monomeric two-state transition, in this case the transition temperature, T_m, is not equal to the temperature at which $\Delta G° = 0$.

The fitted thermodynamic parameters associated with the unfolding of the truncated H2A−H2B dimer as a function of ionic strength (in neutrality) and pH have been summarized in Tables 1 and 2, respectively. The fitted thermodynamic parameters associated with the thermal denaturation of the truncated H3−H4 dimer as a function of ionic strength (at pH 4.5), pH, and protein concentration have been summarized in Tables 3, 4, and 5, respectively.

DISCUSSION

The fact that both truncated H2A−H2B and H3−H4 dimers undergo thermal denaturation as highly cooperative units, without the involvement of any significant population of melting intermediates, is not very surprising, since their full-length counterparts also exhibited two-state folding/unfolding transitions (*9*, *10*). Furthermore, the truncated subunits exhibit very similar stabilities and thermodynamic properties to those of their full-length counterparts under a variety of experimental conditions. A different mechanism of thermal denaturation might have been possible if the removal of the terminal regions of the core histones resulted in major structural rearrangements. This, however, does not appear to be the case since the secondary structures (computed from CD data) of the truncated H2A−H2B dimer and the truncated (H3−H4)/(H3−H4)$_2$ system were very similar to those of the full-length proteins (Figure 10 a,b).

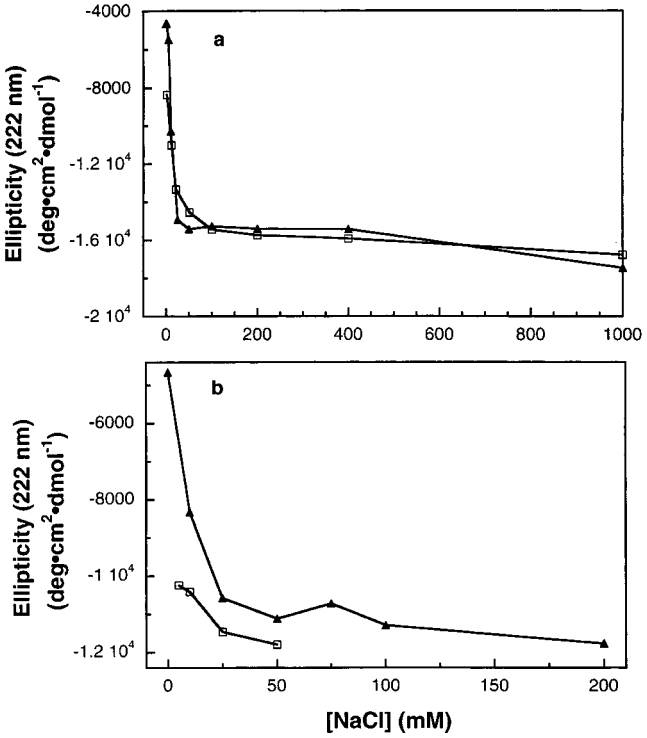

FIGURE 10: (a) Molar ellipticities of the truncated (open squares) and the full-length (filled triangles) H2A−H2B dimers at 222 nm as a function of NaCl concentration. Far-UV CD experiments were performed in 10 mM HEPES, pH 7.5. The protein concentrations were kept constant at 26 μM 11.5-kDa monomer unit and 22 μM 14-kDa monomer unit, respectively. (b) Molar ellipticities of the truncated (open squares) and the full-length (filled triangles) H3−H4 dimers at 222 nm as a function of NaCl concentration. Far-UV CD experiments were performed in 10 mM MES, pH 4.5. The protein concentrations were kept constant at 30 μM 10-kDa monomer unit and 23 μM 13-kDa monomer unit, respectively.

A number of structural studies indicate that the terminal domains of the histone chains are highly unstructured. In most cases, residues 1−15 and 118−128 of H2A, 1−35 of H2B, 1−40 of H3, and 1−20 of H4 are found in unordered conformations (*49*−*55*). These highly unstructured terminal domains of the core histones almost coincide with the peptides that are removed from the histone proteins upon limited trypsinization (*41*, *44*, *45*) and are usually referred to as the labile (or mobile) histone tails. Our results clearly show that the truncated H2A−H2B dimer and the truncated (H3−H4)/(H3−H4)$_2$ system are almost as stable as the full-length complexes and exhibit very similar responses to changes in salt concentration and pH to those of the full-length proteins. Consequently, the more centrally located and structured portions of the polypeptide chains, i.e., the histone fold and the extra-fold structured elements, are the regions responsible for the stability of the assembled states of the core histones, as well as for the effects of ionic strength and pH we have observed. The histone fold is the three-

dimensional structural motif originally identified interstitially within each histone chain by Arents et al. (*53*). It comprises the major portion of the ordered structure of the core histones, and can, thus, be considered the main contributor to the stabilization of these proteins. This architectural motif consists of a long central helix flanked on either side by a loop/β-strand segment and a shorter helix, and is shared by all core histones, despite their low degree of primary sequence homology. The histone fold is involved in the formation of histone heterodimers through the handshake motif of assembly and has been highly conserved through evolution, since it is found in all core histones from archaebacteria to mammals (*56*). In addition, through an extensive search of protein sequence data banks, a consensus primary structure for the histone fold was recently identified in a large number of proteins with diverse functions, e.g., transcription factors, enzymes, etc. (*57*). Therefore, as proposed by Arents and Moudrianakis (*56*), the histone fold emerges as a ubiquitous structural motif utilized in protein dimerization and DNA compaction. The specifics of the histone fold architecture as well as the predictions for its occurrence in proteins other than the canonical histones have been confirmed by several independent studies (*58*, *59*, *54*).

These results clearly demonstrate that the terminal domains of the core histones have only a minor role in the thermodynamic stabilization of the H2A−H2B dimer and the (H3−H4)/(H3−H4)$_2$ system. At low pH and extremely low salt concentrations, the presence of the histone tails is slightly destabilizing, whereas the reverse is true in all other conditions examined. As it is well established, in pure water (or dilute acids), histones exist as individual polypeptides and in the random coil conformation, whereas increasing salt concentrations induce and promote secondary structure (*60*). The highly positively charged terminal sequences of the core histones probably present a competitive element in the initiation of protein folding induced by salt. Therefore, at very low salt concentrations, the truncated histone complexes demonstrate greater overall stability than the full-length proteins. On the other hand, at higher ionic strength conditions the labile histone tails may acquire a partially ordered conformation that contributes to the overall stabilities of the H2A−H2B dimer and the (H3−H4)/(H3−H4)$_2$ system in a minor, but positive, way. In agreement with this idea, an earlier study (*38*) demonstrated that the differences in secondary structure between the truncated and the full-length complexes, although small, became more pronounced at high salt concentrations, with the full-length proteins having increased α-helical and β-structure contents as compared to their truncated counterparts. The presence of the highly charged terminal domains confers an increased solubility to the full-length complexes and thus minimizes the extent of salt-induced protein aggregation. As far as the relatively higher stability of the truncated complexes (especially of the truncated H2A−H2B dimer) at low pH is concerned, trypsin digestion of the core histones essentially coincides with removal of sequences enriched in positively charged residues that require higher pH for stabilization. At the same time, removal of the terminal domains of the core histones probably shifts the isoelectric point of these proteins to lower values, which explains the increased sensitivity to self-aggregation exhibited by the truncated units, H2A−H2B dimer and the (H3−H4)/(H3−H4)$_2$ system, at higher pH.

The terminal domains of the core histones have a minimal effect on the stability of the individual histone complexes, yet are indispensable for life (*61*, *62*, *33*). Thus, from an organizational viewpoint (structural and/or thermodynamic) they must partake in one or more of the following processes: octamer assembly, interactions of octamer with DNA and/or nonhistone chromosomal proteins, and the establishment of higher order chromatin structure. The following examples further support the idea that the histone tails contribute to overall chromatin stability well beyond the level of the stability of the individual octamer subunits. Removal of a pentadecapeptide from the carboxyl terminus of H2A resulted in a partially cleaved H2A−H2B dimer with reduced affinity for the (H3−H4)$_2$ tetramer (*29*). A very thorough and detailed study of the physical properties of selectively truncated nucleosome core particles (*30*) demonstrated that removal of the tails had little effect on the hydrodynamic properties of the core particle in low ionic strength; however, its thermal stability was greatly affected by trypsinization. This result was interpreted as an indication of nucleosome-stabilizing interactions between the histone tails and DNA. Hayes et al. (*32*) demonstrated that removal of the histone tails does not strongly influence the recognition of the nucleosome-positioning sequence elements in the 5SrRNA gene, the extent of bound DNA, or the helical periodicity of DNA in the nucleosome. On the other hand, removal of the histone terminal domains by trypsin was shown to facilitate access of the TFIIIA transcription factor to nucleosomal DNA (*63*, *23*). Finally, a series of elegant studies on the formation of oligonucleosomal arrays and higher order chromatin structure established a definite and specific role of the histone tails in these processes (*64*−*67*) and reviewed by Annunziato and Hansen (*14*).

In conclusion, the results of this study emphasize the central role of the structured domains of the histones (mainly the histone-fold) in the architectural organization and stability of the protein core of the nucleosome. It is these domains that should be considered as the true "endoskeleton" of the gene (*68*). The flexible tails can then be considered as the extensions of this endoskeleton mediating linkages with DNA and with other genome regulatory elements.

REFERENCES

1. Kornberg, R. D. (1974) *Science (Washington, D. C.) 184*, 868.
2. van Holde, K. E. (1988) *Chromatin*, Springer-Verlag, New York.
3. Olins, D. E., Bryan, P. N., Harrington, R. E., Hill, W. E., and Olins, A. L. (1977) *Nucleic Acids Res. 4*, 1911.
4. Weischet, W. O., Tatchell, K., van Holde, K. E., and Klump, H. (1979) *Nucleic Acids Res. 5*, 139.
5. Bina, M., Sturtevant, J. M., and Stein, A. (1980) *Proc. Natl. Acad. Sci. U.S.A. 77*, 4044.
6. Dimitrov, S. I., Dimitrov, R. A., and Tenchov, B. G. (1988) *Int. J. Biol. Macromol. 10*, 149.
7. Balbi, C., Abelmoschi, M. L., Gogioso, L., Parodi, S., Barboro, P., Cavazza, B., and Patrone, E. (1989) *Biochemistry 28*, 3220.
8. Cavazza, B., Brizzolara, G., Lazzarini, G., Patrone, E., Piccardo, M., Barboro, P., Parodi, S., Pasini, A., and Balbi, C. (1991) *Biochemistry 30*, 9060.
9. Karantza, V., Baxevanis, A. D., Freire, E., and Moudrianakis, E. N. (1995) *Biochemistry 34*, 5988.
10. Karantza, V., Freire, E., and Moudrianakis, E. N. (1996) *Biochemistry 35*, 2037.
11. Moore, S. C., and Ausio, J. (1997) *Biochem. Biophys. Res. Commun. 230*, 136.

12. Widom, J. (1998) *Annu. Rev. Biophys. Biomol. Struct. 27*, 285.
13. Leuba, S. H., Bustamante, C., Zlatanova, J., and van Holde, K. (1998) *Biophys. J. 74*, 2823.
14. Annunziato, A. T., and Hansen, J. C. (2000) *Gene Expression 9*, 37.
15. Strahl, B. D., and Allis, C. D. (2000) *Nature 403*, 41.
16. Wu, J., and Grunstein, M. (2000) *Trends Biochem. Sci. 25*, 619.
17. Cheung, P., Allis, C. D., and Sassone-Corsi, P. (2000) *Cell 103*, 263.
18. Shibahara, K., Verreault, A., and Stillman, B. (2000) *Proc. Natl. Acad. Sci. U.S.A. 97*, 7766.
19. Kaufman, P. D., and Almouzni, G. (2000) *Chromatin Structure and Gene Expression*, Oxford University Press, Oxford, 24.
20. Hebbes, T. R., Thorne, A. W., and Crane-Robinson, C. (1988) *EMBO J. 7*, 1395.
21. Kornebrg, R. D., and Lorch, Y. (1992) *Annu. Rev. Cell Biol. 8*, 563.
22. Imhof, A., and Wolffe, A. P. (1998) *Curr. Biol. 8*, R422.
23. Vitolo, J. M., Thiriet, C., Hayes, J. J. (2000) *Mol. Cell. Biol. 20*, 2167.
24. Hörz, W., and Roth, S. (2000) *Chromatin Structure and Gene Expression*, Oxford University Press, Oxford, 49.
25. Logie, C., and Peterson, C. L. (1997) *EMBO J. 16*, 6772.
26. Lorch, Y., Zhang, M., and Kornberg, R. D. (1999) *Cell 96*, 389.
27. Tse, C., Sera, T., Wolffe, A. P., and Hansen, J. C. (1998) *Mol. Cell. Biol. 18*, 4629.
28. Wu, C., Becker, P. B., and Tsukiyama, T. (2000) *Chromatin Structure and Gene Expression*, Oxford University Press, Oxford, 114.
29. Hatch, C. L., Bonner, W. M., and Moudrianakis, E. N. (1983) *Biochemistry 22*, 3016.
30. Eickbush, T. H., Godfrey, J. E., Elia, M. C., and Moudrianakis, E. N. (1988) *J. Biol. Chem. 263*, 18972.
31. Ausio, J., Dong, F., and van Holde, K. E. (1989) *J. Mol. Biol. 206*, 451.
32. Dong, F., Hansen, J. C., and van Holde, K. E. (1990) *Proc. Natl. Acad. Sci. U.S.A.* 87, 5724.
33. Laemmli, U. K. (1970) *Nature (London) 227*, 680.
34. Hayes, J. J., Clark, D. J., and Wolffe, A. P. (1991) *Proc. Natl. Acad. Sci. U.S.A. 88*, 6829.
35. Ling, X., Harkness, T. A., Schultz, M. C., Fisher-Adams, G., and Grunstein, M. (1996) *Genes Dev. 10*, 686.
36. Turner, B. M. (1991) *J. Cell Sci. 99*, 13.
37. Nowak, S. J., and Corces, V. G. (2000) *Genes Dev. 14*, 3003.
38. Nakayama, J., Rice, J. C., Strahl, B. D., Allis, C. D., and Grewal, S. I. (2001) *Science 292*, 110.
39. Eickbush, T. H., and Moudrianakis, E. N. (1978) *Biochemistry 17*, 4955.
40. Godfrey, J. E., Baxevanis, A. D., and Moudrianakis, E. N. (1990) *Biochemistry 29*, 8817.
41. Weintraub, H., and van Lente, F. (1974) *Proc. Natl. Acad. Sci. U.S.A. 71*, 4249.
42. Böhm, L., Briand, G., Sautiere, P., and Crane-Robinson, C. (1981) *Eur. J. Biochem. 119*, 67.
43. Whitlock, J. P., Jr., and Stein, A. (1978) *J. Biol. Chem. 253*, 3857.
44. Lilley, D. M. J., and Tatchell, K. (1977) *Nucleic Acids Res. 4*, 2039.
45. Tatchell, K., and van Holde, K. E. (1977) *Biochemistry 16*, 5295.
46. Böhm, L., Crane-Robinson, C., and Sautiere, P. (1980) *Eur. J. Biochem. 106*, 525.
47. Böhm, L., Briand, G., Sautiere, P., and Crane-Robinson, C. (1982) *Eur. J. Biochem. 123*, 299.
48. Freire, E. (1989) *Comments Mol. Cell. Biophys. 6*, 123.
49. Ramsay, G., and Freire, E. (1990) *Biochemistry 29*, 8677.
50. Thompson, K. S., Vinson, C. R., and Freire, E. (1993) *Biochemistry 32*, 5491.
51. Bradbury, E. M., and Rattle, H. W. E. (1972) *Eur. J. Biochem. 27*, 270.
52. Bradbury, E. M., Cary, P. D., Crane-Robinson, C., and Rattle, H. W. E. (1973) *Ann. N. Y. Acad. Sci. 222*, 266.
53. Moss, T., Cary, P. D., Crane-Robinson, C., and Bradbury, E. N. (1976) *Biochemistry 15*, 2261.
54. Smith, R. M., and Rill, R. L. (1989) *J. Biol. Chem. 264*, 10574.
55. Arents, G., Burlingame, R. W., Wang, B.-C., Love, W. E., and Moudrianakis, E. N. (1991) *Proc. Natl. Acad. Sci. U.S.A. 88*, 10148.
56. Luger, K., Mader, A. W., Richmond, R. K., Sargent, D. F., and Richmond, T. J. (1997) *Nature 389*, 231.
57. Dutnall, R. N., and Ramakrishnan, V. (1997) *Structure 5*, 1255.
58. Arents, G., and Moudrianakis, E. N. (1995) *Proc. Natl. Acad. Sci. U.S.A. 92*, 11170.
59. Baxevanis, A. D., Arents, G., Moudrianakis, E. N., and Landsman, D. (1995) *Nucleic Acids Res. 23*, 2685.
60. Xie, X., Kokubo, T., Cohen, S. L., Mirza, U. A., Hoffmann, A., Chait, B. T., Roeder, R. G., Nakatani, Y., and Burley, S. K. (1996) *Nature 380*, 316.
61. Starich, M. R., Sandman, K., Reeve, J. N., and Summers, M. F. (1996) *J. Mol. Biol. 255*, 187.
62. Isenberg, I. (1979) *Annu. Rev. Biochem. 48*, 159.
63. Kayne, P. S., Kim, U. J., Han, M., Mullen J. R., Yoshizaki, F., and Grunstein, M. (1988) *Cell 55*, 27.
64. Morgan, B. A., Mittman, B. A., and Smith, M. M. (1991) *Mol. Cell. Biol. 11*, 4111.
65. Lee, D. Y., Hayes, J. J., Pruss, D., and Wolffe, A. P. (1993) *Cell 72*, 73.
66. Allan, J., Harborne, N., Rau, D. C., and Gould, H. (1982) *J. Cell Biol. 93*, 285.
67. Garcia-Ramirez, M., Dong, F., and Ausio, J. (1992) *J. Biol. Chem. 267*, 19587.
68. Fletcher, T. M., and Hansen, J. C. (1995) *J. Biol. Chem. 270*, 25359.
69. Schwarz, P. M., Fletcher, T. M., Felthasuer, A., and Hansen, J. C. (1996) *Biochemistry 35*, 4009.
70. Arents, G., and Moudrianakis, E. N. (1993) *Proc. Natl. Acad. Sci. U.S.A. 90*, 10489.

BI0110140